




Synthesis of Ni, N co-doped TiO₂ using microwave-assisted method for sodium lauryl sulfate degradation by photocatalyst

Muhammad Nurdin , La Ode Ahmad Nur Ramadhan, Darmawati Darmawati, Maulidiyah Maulidiyah , Dwipayogo Wibowo 

© American Coatings Association 2017

Abstract A titanium dioxide (TiO₂) photocatalyst was modified with nickel (Ni) and nitrogen (N) in titanium tetra-isopropoxide (TTIP) as a precursor through a microwave-assisted method. The Ni and N dopants led to a decrease in the TiO₂ band gap and made it able to function with visible light irradiation. The results of X-ray diffraction analysis demonstrated that the crystalline size of Ni–N–TiO₂ was 13.275 nm in anatase form with a specific peak in $2\theta = 25.32^\circ$. Ni–N–TiO₂ was analyzed by scanning electron microscopy, which showed the smaller morphology and thin particles, and this was further supported by energy-dispersive X-ray data regarding the elemental composition of Ni and N being 4.50 and 2.39%, respectively. Fourier transform infrared spectroscopy results demonstrated the absorption spectrum in wavenumbers of 1197 and 1149 cm⁻¹, indicating an N–TiO₂ bond, a Ti–O bond at 648 cm⁻¹, and an Ni–O bond at 469 cm⁻¹. TiO₂ modified by Ni and N exhibited a decrease in the band gap at 1.95 eV, suggesting the Ni and N dopants successfully inserted onto the TiO₂ crystalline surface to be visualized with visible light. Photoactivity testing was carried out to degrade sodium lauryl sulfate surfactants under visible irradiation, where the degradation efficiency was 93.75%.

Keywords Photocatalyst, TiO₂, Nitrogen, Nickel, Surfactant, Microwave assisted

M. Nurdin (✉), L. O. A. N. Ramadhan, D. Darmawati, M. Maulidiyah, D. Wibowo
Department of Chemistry, Faculty of Mathematics and Natural Sciences, Universitas Halu Oleo, Jl. HEA Mokodompit Kampus Baru UHO, Kendari 93232, Southeast Sulawesi, Indonesia
e-mails: mnurdin06@yahoo.com, muhammad.nurdin@uho.ac.id

Introduction

Surfactant waste processing requires serious attention in nature where human life can be endangered, such as with rivers, groundwater, and sediment pollutions.¹ One of the major pollutant types in water is sodium lauryl sulfate (SLS), an anionic surfactant category that comprises detergents, toothpaste, and shampoo.² SLS can degrade naturally in aerobic conditions (sufficient oxygen and microorganisms) and with UV light irradiation from sunlight, degradation requires a long time to take place.^{3,4}

The technology necessary for wastewater treatment development over the last decade is represented by photocatalysis, one of the most promising technologies because it quickly and safely makes use of oxidation and reduction reactions under light irradiation.^{5,6} There are certain semiconductor types used for the photocatalytic processes, such as TiO₂, CdS, ZnO, GaP, SiC, and Fe₂O₃.⁷ TiO₂ is a semiconductor that has attracted much attention because it has high photocatalytic activity and is nontoxic and resistant to corrosion, not dissolving in water.⁸ TiO₂ can be found in nature in metamorphic and igneous rocks known as ilmenite (FeO·TiO₂).^{9,10} In addition, TiO₂ can degrade organic waste and dyes while also acting as a disinfectant for medical equipment.¹¹ A TiO₂ semiconductor is only active under UV light conditions because it has a band gap energy of 3.2 eV.^{12,13} This is a constraint when utilizing sunlight because UV light abundance is just 10%.^{14,15} There are efforts regarding the improvement of TiO₂ photocatalysis by shifting the band gap energy so that it is active under visible light by modifying via insertion of metals and nonmetals.¹⁶

A nonmetallic dopant is generally added to TiO₂, i.e., nitrogen (N),¹² carbon (C),¹⁷ sulfur (S),¹⁸ phosphorus (P),^{19,20} and fluorine (F),²¹ but N as a dopant is more effective because it has an atomic size that is the same as oxygen (O) and a low ionization energy.²² A

number of studies have also shown that using transition metal dopants, such as Fe, La, Ni, Mn, Au, or Ag, to decrease the band gap and to improve photocatalytic activity in the visible light region is possible.^{23–26} A transition metal dopant in TiO₂ can serve as an electron trap to improve electron–hole pair separation.²⁷

This study examined Ni and N co-doped within a TiO₂ catalyst process using a microwave-assisted method because it has the benefits of being environmentally friendly and energy efficient. The improved particle kinetics through the microwave-assisted synthesis of the material was observed in a relatively short time with lower energy consumption,²⁸ so it was considered a quite promising method for the modification of TiO₂ photocatalysts

Experimental

Preparation of Ni–N–TiO₂

The preparation of Ni and N was done by the sol–gel method. These were made by two solutions (A and B). For solution A: 8 mL TTIP was put in 1 mL of acetylacetone containing 30 mL ethanol and for solution B: 30 mL ethanol was put in 4 mL of distilled water containing 2 mL glacial acetic acids. The two solutions were mixed to obtain the TiO₂ sol. The sol was added to 30 mL of 1 M urea solution. Then, it was added by Ni(NO₃)₂·6H₂O with the ratio of 1%, 3%, 5%, and 7%. Subsequently, the solution was heated in a microwave for 30 min. Finally, it was washed with distilled water, filtered, and dried in an oven at 100°C, then calcined at 500°C for 1.5 h to obtain the Ni–N–TiO₂ crystal.

Characterization of the synthesized Ni–N–TiO₂

The surface morphology of the synthesized Ni–N–TiO₂ crystal was observed using SEM (JEOL, Model 5900LV). The surface composition was analyzed by EDS (Oxford Links ISIS) and the FTIR spectra by Jasco FT/IR 6600. The band gap was obtained by LAMBDA 950 UV–Vis spectrophotometer PerkinElmer, and the X-ray diffraction spectra of the Ni–N–TiO₂ were obtained using a Philips PW 1050–3710 diffractometer under Cu Ka radiation.

Preparation of SLS solutions

Preparation of SLS solution consists of 0.4, 0.8, 1.2, and 1.4 mg/L. The 3 mL of SLS solution with a concentration of 0.4 mg/L was extracted using separating funnel by adding 5 mL methylene blue and 2 mL chloroform for 30 min. Phases of chloroform were combined and absorbance measured at a wavelength of 640–659 nm

using a UV–Vis spectrophotometer to obtain a wavelength maximum from SLS.

Degradation test of SLS solutions

The degradation test of SLS was performed by using 300 mg of catalysts added into 400 mL SLS with concentrations of 0.4, 0.8, 1.2, and 1.4 mg/L, respectively. The photocatalysts processed for 120 min with irradiation by visible light (Philips Halogen lamp 150 W Halolite) and were analyzed by using a UV–Vis spectrophotometer. The absorbance values have integrated into the linear regression equation: $y = ax + b$, to obtain the concentration and percentage of sample degradation of the measurement with:

$$\%D = \frac{C_0 - C_1}{C_0} \times 100\%$$

where % D is the percentage of SLS concentration degradation, C₀ the initial concentration of SLS, and C₁ the concentration degraded of SLS.

Results and discussion

Preparation of Ni–N–TiO₂ catalyst

In this research, the kinetics of molecules was improved with microwave assistance at a power of 450 watts for 30 min based on Jaimy et al.²⁹ The composition variations of Ni dopant were obtained by the addition effects of Ni on TiO₂ photocatalytic activity. The hydrothermal treatment was calcined at 500°C for 1.5 h to obtain a TiO₂ powder with an anatase crystalline structure that was advantageous in terms of photocatalytic activity.³⁰ Table 1 lists the physical properties of the material synthesized photocatalyst, where the addition of Ni and N dopants also increased the yield to an optimum of 83.17% Ni(1%)–N–TiO₂.

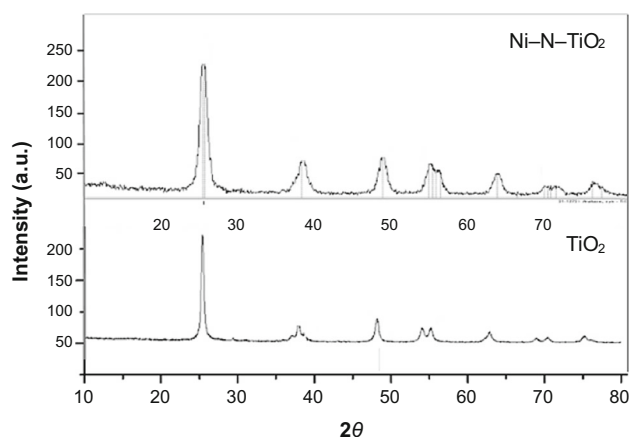
Characterization of Ni–N–TiO₂ catalyst

X-ray diffraction (XRD)

Characterization by XRD to obtain data on the Ni–N–TiO₂ crystal structure was performed. Figure 1 shows 17 peaks in the XRD pattern of Ni–N–TiO₂, specifically $2\theta = 25.32^\circ, 25.52^\circ, 37.88^\circ, 44.011^\circ, 48.16^\circ, 53.922^\circ, 54.42^\circ, 54.9^\circ, 55.44^\circ, 62.64^\circ, 65.22^\circ, 68.623^\circ, 69.106^\circ, 69.515^\circ, 70.165^\circ, 74.782^\circ, \text{ and } 76.02^\circ$. The XRD data demonstrated that the Ni and N dopants were distributed in the lattice of anatase, seen at $2\theta = 25.3^\circ; 37.9^\circ, 48.1^\circ, 54^\circ, 54.9^\circ, 62.6^\circ, 69.05^\circ, 70.1^\circ, 75.2^\circ, \text{ and } 82.7^\circ$, with field diffractions of (101), (004), (200), (105), (211), and (204), respectively. Crystal anatase

Table 1: The physical properties of the material synthesized by using microwave-assisted hydrothermal method

Catalysts	Color	Mass (g)	Yield (%)
TiO ₂	White	1.732	82.74
N-TiO ₂	Light brown	2.084	82.91
Ni-TiO ₂	Light yellow	1.822	82.88
Ni(1%)-N-TiO ₂	Light yellow	2.108	83.17
Ni(3%)-N-TiO ₂	Light yellow	2.138	82.98
Ni(5%)-N-TiO ₂	Light yellow	2.171	82.91
Ni(7%)-N-TiO ₂	Light yellow	2.198	82.62

**Fig. 1: The result of XRD pattern on Ni-N-TiO₂ catalyst**

(101) had a robust influence on TiO₂ photocatalytic activity. According to Nurdin et al.,²⁴ the TiO₂ anatase has the large surface area to enhance the high photocatalytic activity. It can be calculated using the Scherer equation.

$$D = \frac{0.9\lambda}{\beta \cos \theta}$$

where D is crystal size (nm), λ is the wavelength of the X-ray (0.15406 nm), β is the half width of the diffraction peak (rad), and θ is the angle of the diffraction peaks (°). From the Scherer equation, the obtained TiO₂ crystal size was 13.275 nm.

UV-Vis diffuse reflectance spectroscopy (UV-Vis DRS)

UV-Vis DRS was employed to obtain the band gap of synthesized Ni-N-TiO₂. The higher the band gap value, the greater was the effect on semiconductor performance that was observed because there was still the requirement for large amounts of energy to excite the electrons from the valence band to the conduction band. The presence of Ni and N dopants was very effective in increasing TiO₂ performance because these dopants could separate the electron-hole from the valence band onto the conduction band. The band gap

of Ni-N-TiO₂ was calculated by using the Kubelka-Munk factor [F(R)], with the band gap value of 1.9534 eV (Fig. 2). This was smaller than the pure TiO₂ (3.2 eV),³¹ N (2.6 eV),¹² and Ni (2.33 eV).³² The successful Ni-N-TiO₂ synthesis using a microwave-assisted method demonstrated that there was a smaller band gap than conventional methods of 2.28 eV.³³ This was caused by the microwave-assisted where the material receives energy emitted to accelerate the reaction. The decrease in the band gap value to form the photo hole (valence band) and photoelectron (conduction band) in visible light was influenced by the dopants.

Based on Ruslan et al.,²⁵ the band gap can be used to calculate the corresponding wavelength (UV-Vis) spectra regions by Plank-Einstein relation [$E = hc/\lambda = (1239.8 \text{ eV nm})/\lambda$]. In this study, the synthesized Ni-N-TiO₂ has been activated in visible wavelength regions at 634.68 nm.

Fourier transform infrared spectroscopy (FTIR)

FTIR measurements were carried out to identify the formation of the bond with Ti, N, Ni, and O as the resulting effect of adding Ni and N dopants to TiO₂.

The wavenumber at 1197 and 1149 cm⁻¹ was indicative of the N-TiO₂ bonds. The absorption at wavenumber of 648 cm⁻¹ and 469 cm⁻¹ were presented a Ti-O and Ni-O bonds, respectively. According to Ruslan et al.²⁵ the vibration of the metal with an O group was expected to appear at the wave number 600-400 cm⁻¹ (Fig. 3).

Scanning electron microscopy energy-dispersive x-ray (SEM-EDX)

The SEM-EDX measurement results were utilized to explain the surface morphology from the elements on the Ni-N-TiO₂ catalyst. Figure 4 shows the morphology measurements of the TiO₂ and Ni-N-TiO₂ catalysts.

Figure 4a is a morphology of TiO₂ synthesized by the sol-gel method, while Fig. 4b is the physical changes of the Ni-N-TiO₂ that had a smaller size than TiO₂. The smaller particle size was obtained with the large active surface area on the photocatalyst. It

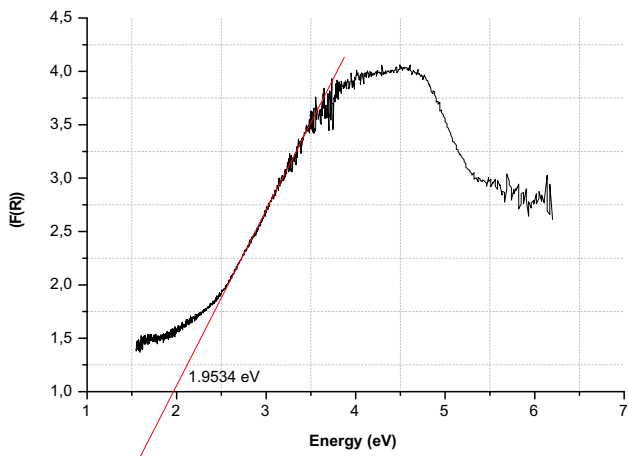


Fig. 2: The result of band gap of Ni-N-TiO₂ catalyst

permitted collisions with the materials to be a catalyst for the rapid reaction.

The composition of the catalyst using the EDX catalyst meant that Ni-N-TiO₂ possessed atoms of C, O, N, Ti, and Ni at proportions of 6.04, 34.94, 2.39, 52.12, and 4.5%, respectively (Fig. 5).

Degradation test using SLS solution

Effect of dopants nitrogen (N) and nickel (Ni) on the performance of TiO₂ catalyst

The addition of dopants into the TiO₂ matrix showed that TiO₂ can be active under visible light such that the SLS surfactant is degraded as can be seen in Fig. 6. The presence of the N dopant in TiO₂ im-

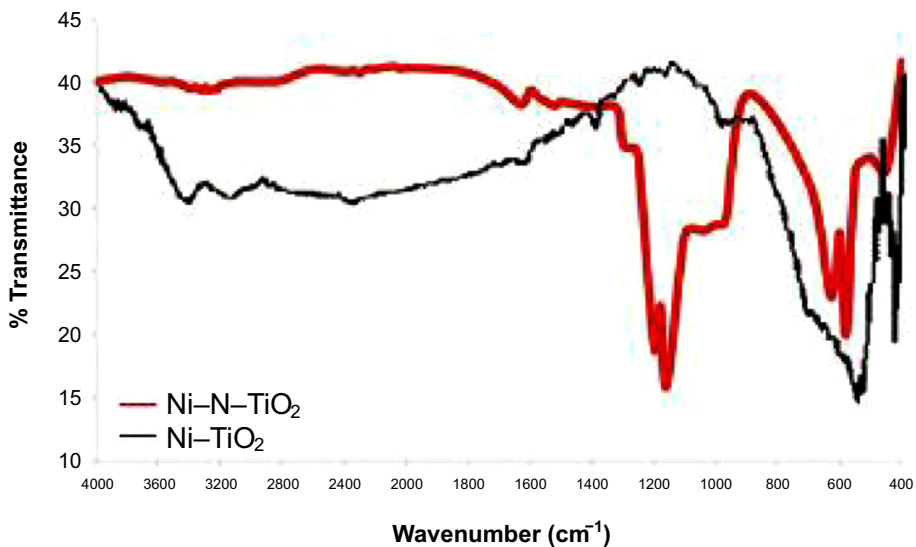


Fig. 3: FTIR spectra of Ni-N-TiO₂ and Ni-TiO₂ catalysts

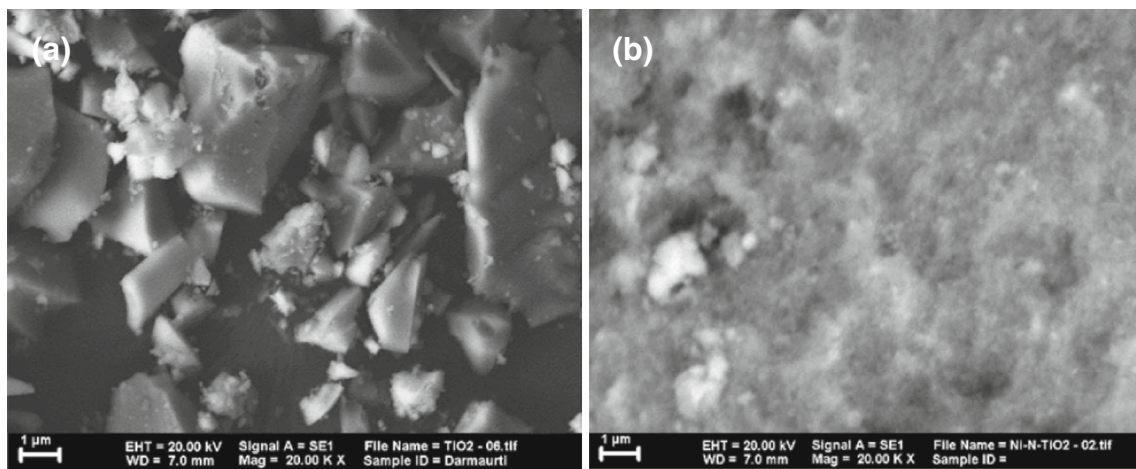


Fig. 4: The morphology of catalysts in scale bar: 1 μm; (a) TiO₂, and (b) Ni-N-TiO₂

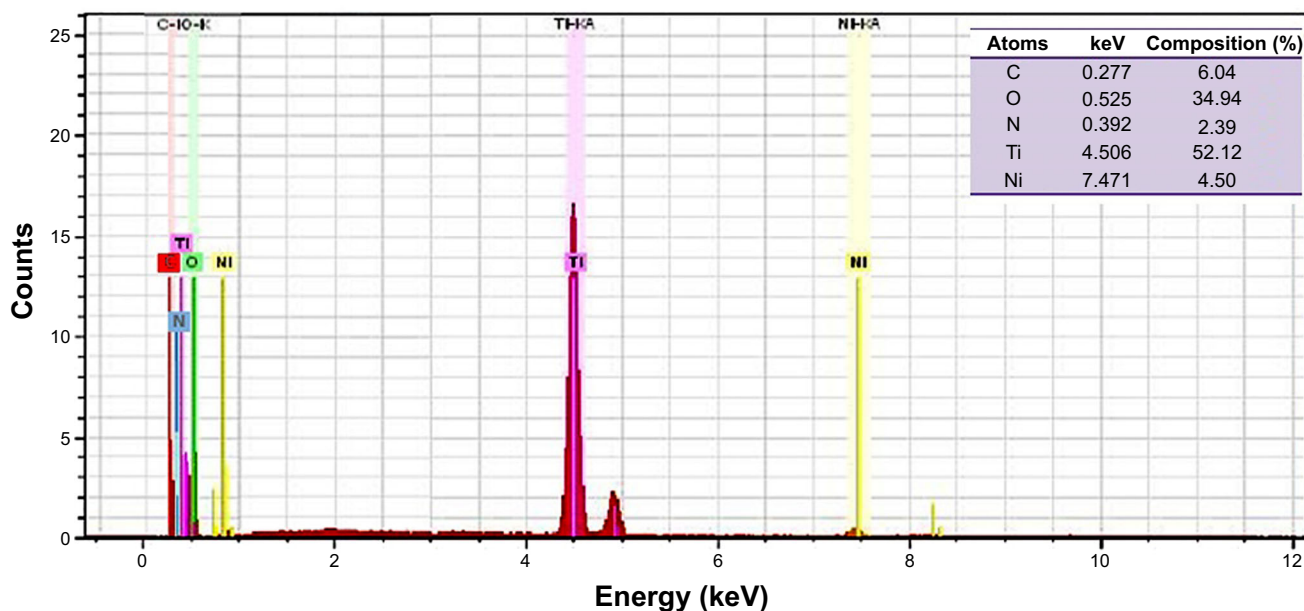


Fig. 5: The result of EDX spectrum on Ni-N-TiO₂ catalyst

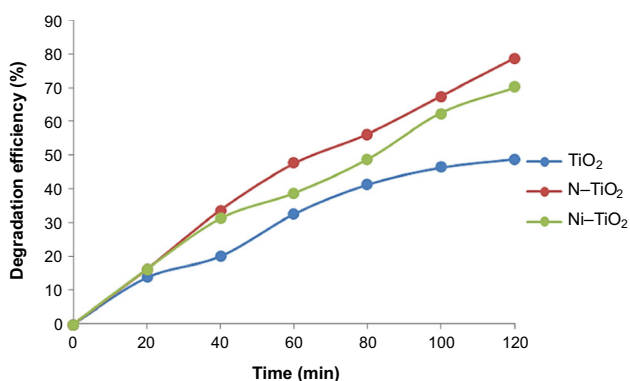


Fig. 6: The performance test comparison on TiO₂ dopants to degrade SLS in visible light combined of TiO₂, N-TiO₂ and Ni-TiO₂ catalysts

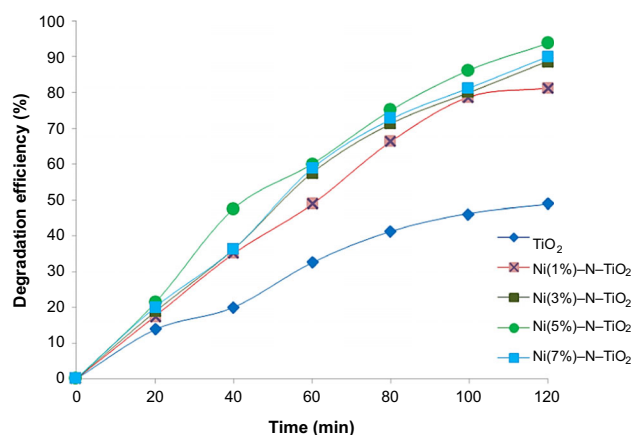


Fig. 7: The composition effect of Ni dopant in N-TiO₂ to degrade 0.8 mg/L SLS under visible light

proved the degradation efficiency of the SLS surfactant by 78.75% compared to the standard TiO₂ catalyst (48.75%). According to Asahi et al.,³⁴ the mixing of the p states on the N dopant with O in the 2p valence band could decrease the TiO₂ band gap, while the conduction band is steady state position. SLS degradation was obtained using TiO₂ dopant Ni under visible light irradiation with the efficiency of 70% compared with the standard TiO₂ photocatalyst.

Effect variation of nickel (Ni) dopants

The effect of the Ni dopant at composition variations of 1, 3, 5, and 7% to degrade SLS through Ni-N-TiO₂

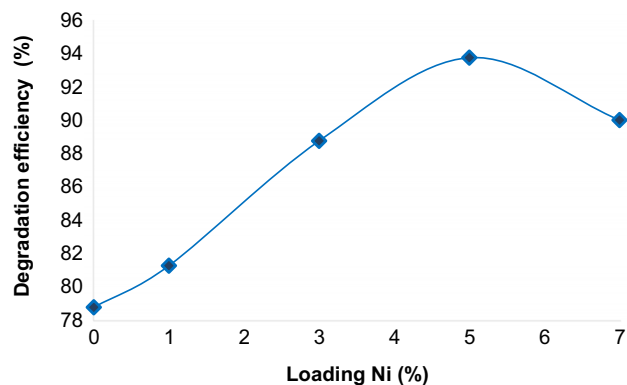


Fig. 8: The loading effect of Ni dopant to degrade the 0.8 mg/L SLS surfactant in visible light irradiation for 120 min

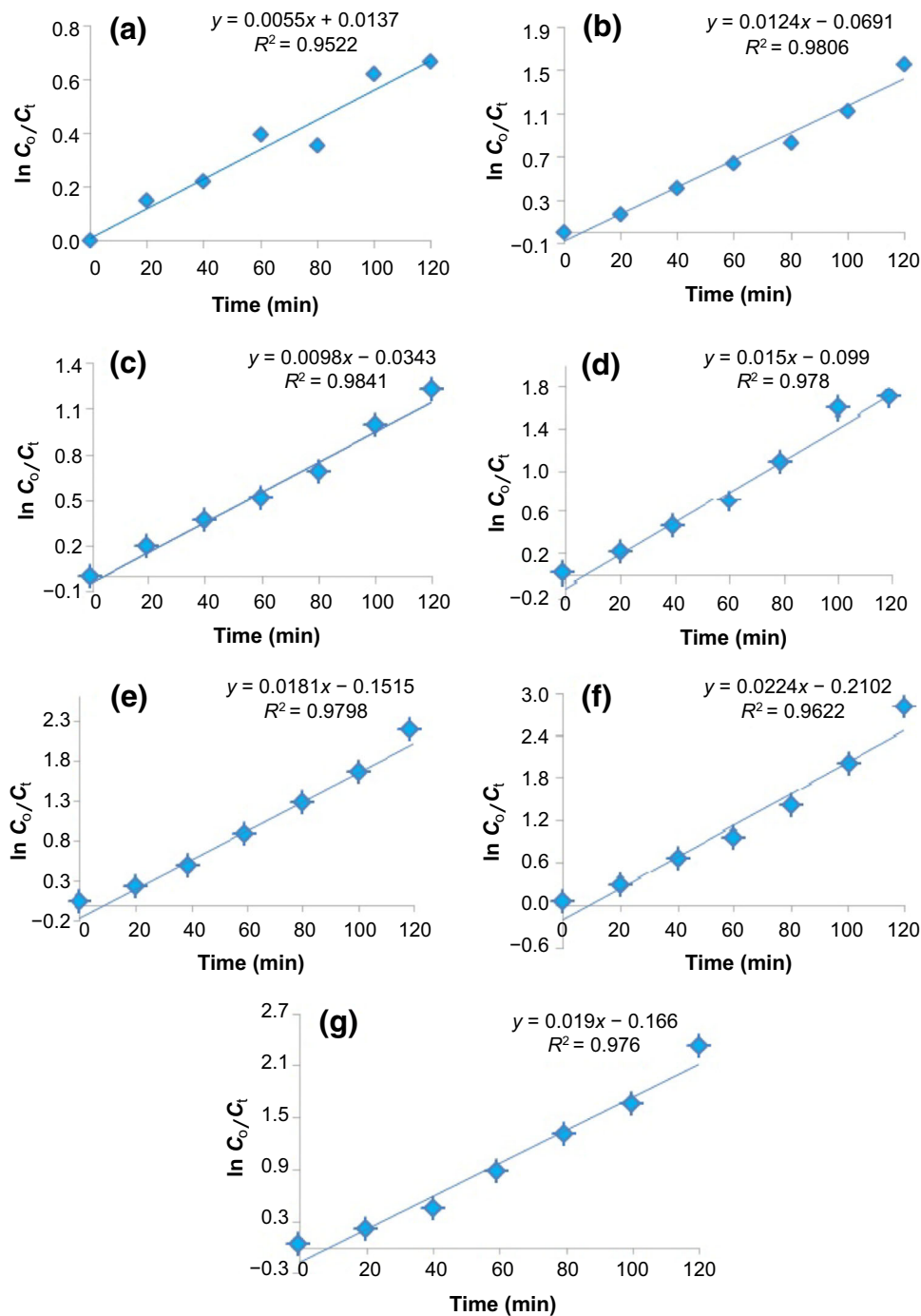


Fig. 9: The kinetics rate of SLS degradation kinetics at 0.8 mg/L using the photocatalyst (a) TiO_2 , (b) N-TiO_2 , (c) Ni-TiO_2 , (d) Ni(1\%)-N-TiO_2 , (e) Ni(3\%)-N-TiO_2 , (f) Ni(5\%)-N-TiO_2 , (g) Ni(7\%)-N-TiO_2

photocatalysis exhibited the most optimal degradation results in 120 min at 5% loading of Ni with the degradation equivalent to 93.75% (Fig. 7).

Zhang et al.³⁵ noted that a metal dopant was inserted into the N-TiO_2 system as an electron trap that enhances photocatalytic activity. Meanwhile, a dopant is required at a precise composition in N-TiO_2 for SLS degradation. This was observed for Ni-N-

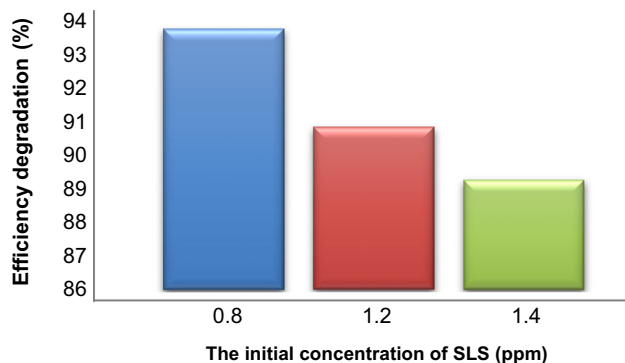
TiO_2 at 5%, and the specific Ni loading is shown in Fig. 8.

Rate constant for SLS degradation test

The reaction rate constant and reactant concentrations can be determined by examining the reactant concen-

Table 2: The reaction rate constant of SLS degradation on 0.8 mg/L

Variable	k (mg L ⁻¹ /min)
SLS + TiO ₂	0.0055
SLS + N-TiO ₂	0.0124
SLS + Ni-TiO ₂	0.0098
SLS + Ni(1%)-N-TiO ₂	0.0150
SLS + Ni(3%)-N-TiO ₂	0.0181
SLS + Ni(5%)-N-TiO ₂	0.0227
SLS + Ni(7%)-N-TiO ₂	0.0190

**Fig. 10: The initial concentration effect of SLS against efficiency degradation**

tration at any time during the reaction. If a reaction occurs at very low concentrations (mg L⁻¹), the reaction takes place as a first-order reaction, i.e.,

$$\ln \frac{[C_0]}{[C]} = kt$$

where C_0 is a concentration during the time of degradation at $t = 0$, C is the concentration during the time of degradation at $t = t$, k is the reaction rate constant, and t is the time in minutes. $\ln \frac{[C_0]}{[C]}$ is plotted against time of irradiation (t) to obtain linear curves with a k slope¹⁶ as shown in Fig. 9.

Table 2 lists the reaction rate constant for SLS by Ni(5%)-N-TiO₂ which is greater than TiO₂ catalyst, N-TiO₂, Ni-TiO₂, and Ni-N-TiO₂ with the loading of Ni at the same time. The rate of the reaction using the Ni-N-TiO₂ catalyst with 5% Ni loading was faster in degrading SLS (Fig. 10).

Variation effect of initial concentration on SLS degradation

The variable effect of initial concentration on SLS degradation using Ni(5%)-N-TiO₂ with SLS concentrations of 0.8 mg/L, 1.2 mg/L, and 1.4 mg/L demon-

strated optimum degradation at 93.75, 90.83, and 1.4%, respectively.

When the initial concentration increased, surfactant molecules are adsorbed on the catalyst surface. However, when the molecules are adsorbed on the catalyst, the SLS surfactant does not entirely degrade because of the light intensity and catalyst constant factors.³⁶ The high concentrations of SLS on the catalyst surface decrease the production of $\cdot\text{OH}$ on the catalyst. Furthermore, the SLS solution will absorb many photons, causing their availability for activation of the catalyst to be reduced.

Conclusion

Modified TiO₂ nanoparticles were successfully synthesized using a microwave-assisted method to produce a photocatalytic material in an anatase crystalline form with a size of 13.27 nm. The Ni and N dopants in TiO₂ decreased the band gap energy of 1.9534 eV—the material could be activated by visible light. The TiO₂ photocatalyst with Ni and N dopants improved catalytic performance in degrading SLS up to 81.25% for Ni(1%)-N-TiO₂, 88.75% for Ni(3%)-N-TiO₂, 93.75% for Ni(5%)-N-TiO₂, and 90.00% for Ni(7%)-N-TiO₂. Furthermore, TiO₂, N-TiO₂, and Ni-TiO₂ as photocatalysts had degradation efficiencies of 48.75, 78.75, and 70.0%, respectively.

Acknowledgment We acknowledge the financial support of the DRPM—Ministry of Research, Technology and Higher Education, the Republic of Indonesia.

References

1. Giacco, TD, Germani, R, Saracino, F, Stradiotto, M, “Counterion Effect of Cationic Surfactants on the Oxidative Degradation of Alizarin Red-S Photocatalysed by TiO₂ in Aqueous Dispersion.” *J. Photochem. Photobiol. A Chem.*, **332** 546–553 (2017)
2. Mehling, A, Kleber, M, Hensen, H, “Comparative Studies on the Ocular and Dermal Irritation Potential of Surfactants.” *Food Chem. Toxicol.*, **45** 747–758 (2007)
3. Nam, W, Woo, K, Han, GY, “Photooxidation of Anionic Surfactant (Sodium Lauryl Sulfate) in a Three-Phase Fluidized Bed Reactor Using TiO₂/SiO₂ Photocatalyst.” *J. Ind. Eng. Chem.*, **15** 348–353 (2009)
4. Nurdin, M, Maulidiyah, “Fabrication of TiO₂/Ti Nanotube Electrode by Anodizing Method and Its Application on Photoelectrocatalytic System.” *Int. J. Sci. Technol. Res.*, **3** (2) 122–126 (2014)
5. Nurdin, M, Wibowo, W, Supriono, Febrian MB, Surahman, H, Krisnandi, YK, Gunlazuardi, J, “Pengembangan Metode Baru Penentuan Chemical Oxygen Demand (COD) Berbasis Sel Fotoelektrokimia: Karakterisasi Elektroda Kerja Lapis Tipis TiO₂/ITO.” *Makara Sains*, **13** (1) 1–8 (2009)

6. Nurdin, M, "Preparation, Characterization and Photoelectrocatalytic Activity of Cu@N-TiO₂/Ti Thin Film Electrode." *Int. J. Pharma Bio Sci.*, **5** (3) 360–369 (2014)
7. Wang, W-N, An, W-J, Ramalingan, B, Mukherjee, S, Niedzwiedzki, DM, Gangopadhyay, S, Biswas, P, *J. Am. Chem. Soc.*, **134** 11276–11281 (2012)
8. Maulidiyah, Nurdin, M, Erasmus, Wibowo D, Natsir, M, Ritonga, H, Watoni, AH, "Probe Design of Chemical Oxygen Demand (COD) Based on Photoelectrocatalytic and Study of Photocurrent Formation at SnO-F/TiO₂ Thin Layer by Using Amperometry Method." *Int. J. Chemtech Res.*, **8** (1) 416–423 (2015)
9. Nurdin, M, Maulidiyah, Watoni, AH, Abdillah, N, Wibowo, D, "Development of Extraction Method and Characterization of TiO₂ Mineral from Ilmenite." *Int. J. Chemtech Res.*, **9** (4) 483–491 (2016)
10. Nurdin, M, Zaeni, A, Maulidiyah, Natsir, M, Bampe, A, Wibowo, D, "Comparison of Conventional and Microwave-Assisted Extraction Methods for TiO₂ Recovery in Mineral Sands." *Orient. J. Chem.*, **32** (5) 2713–2721 (2016)
11. Maulidiyah, Ritonga, H, Salamba, R, Wibowo, D, Nurdin, M, "Organic Compound Rhodamine B Degradation by TiO₂/Ti Electrode in a New Portable Reactor." *Int. J. Chemtech Res.*, **8** (6) 645–653 (2015)
12. Maulidiyah, Nurdin, M, Widianingsih, E, Azis, T, Wibowo, D, "Preparation of Visible Photocatalyst N-TiO₂ and Its Activity on Congo Red Degradation." *ARPJ J. Eng. Appl. Sci.*, **10** (15) 6250–6256 (2015)
13. Maulidiyah, Ritonga, H, Faiqoh, CE, Wibowo, D, Nurdin, M, "Preparation of TiO₂-PEG Thin Film on Hydrophilicity Performance and Photocurrent Response." *Biosci., Biotechnol. Res. Asia*, **12** (3) 1985–1989 (2015)
14. Maulidiyah, Tribawono, DS, Wibowo, D, Nurdin, M, "Electrochemical Profile Degradation of Amino Acid by Flow System Using TiO₂/Ti Nanotubes Electrode." *Anal. Bioanal. Electrochem.*, **8** (6) 761–776 (2016)
15. Leijtens, T, Eperon, GE, Pathak, S, Abate, A, Lee, MM, Snaith, HJ, "Overcoming Ultraviolet Light Instability of Sensitized TiO₂ with Meso-Superstructured Organometal Tri-Halide Perovskite Solar Cells." *Nat. Commun.*, **4** 1–8 (2013)
16. Maulidiyah, Nurdin, M, Wibowo, D, Sani, A, "Nanotube Titanium Dioxide/Titanium Electrode Fabrication with Nitrogen and Silver Metal Doped Anodizing Method: Performance Test of Organic Compound Rhodamine B Degradation." *Int. J. Pharm. Pharm. Sci.*, **7** (6) 141–146 (2015)
17. Maulidiyah, Wibowo, D, Hikmawati, Salamba R, Nurdin, M, "Preparation and Characterization of Activated Carbon from Coconut Shell—Doped TiO₂ in Water Medium." *Orient. J. Chem.*, **31** (4) 2337–2342 (2015)
18. Lin, Y-H, Hsueh, H-T, Chang, C-W, Chu, H, "The Visible Light-Driven Photodegradation of Dimethyl Sulfide on S-Doped TiO₂: Characterization, Kinetics, and Reaction Pathways." *Appl. Catal. B*, **199** 1–10 (2016)
19. Viaano, V, Sacco, O, Lervolino, G, Sannino, D, Ciambelli, P, Liguori, R, Bezzeccheri, E, Rubino, A, "Enhanced Visible Light Photocatalytic Activity by Up-Conversion Phosphors Modified N-Doped TiO₂." *Appl. Catal. B*, **176** 594–600 (2015)
20. Wang, K, Yu, J, Liu, L, Hou, L, Jin, F, "Hierarchical P-Doped TiO₂ Nanotubes Array@Ti Plate: Towards Advanced CO₂ Photocatalytic Reduction Catalysts." *Ceram. Int.*, **42** (14) 16405–16411 (2016)
21. Guo, Q, Zhang, Z, Ma, X, Jing, K, Shen, M, Yu, N, Tang, J, Dionysiou, DD, "Preparation of N, F-Codoped TiO₂ Nanoparticles by Three Different Methods and Comparison of Visible-Light Photocatalytic Performances." *Sep. Purif. Technol.*, **175** 305–313 (2017)
22. Cong, Y, Zhang, J, Chen, F, Anpo, M, "Synthesis and Characterization of Nitrogen-Doped TiO₂ Nanophotocatalyst with High Visible Light Activity." *J. Phys. Chem. C*, **111** 6976–6982 (2007)
23. Yeganeh, M, Shahtahmasebi, N, Kompany, A, Karimipour, M, Razali, F, Nasralla, NHS, Siller, L, "The Magnetic Characterization of Fe Doped TiO₂ Semiconducting Oxide Nanoparticles Synthesized by Sol-Gel Method." *Phys. B*, **511** 89–98 (2017)
24. Nurdin, M, Muzakkar, MZ, Maulidiyah, M, Maulidiyah, N, Wibowo, D, "Plasmonic Silver—N/TiO₂ Effect on Photoelectrocatalytic Oxidation Reaction." *J. Mater. Environ. Sci.*, **7** (9) 3334–3343 (2016)
25. Ruslan, Mirzan M, Nurdin, M, Wahab, AW, "Characterization and Photocurrent Response of Mn-N-TiO₂/Ti Electrode: Approach for Chemical Oxygen Demand (COD) Sensor." *Int. J. Appl. Chem.*, **12** (3) 399–409 (2016)
26. Arham, Z, Nurdin, M, Buchari, B, "Photoelectrocatalysis Performance of La₂O₃ doped TiO₂/Ti Electrode in Degradation of Rhodamine B Organic Compound." *Int. J. Chemtech Res.*, **9** (11) 113–120 (2016)
27. Choi, W, Termin, A, Hoffmann, MR, "The Role of Metal Ion Dopants in Quantum-Sized TiO₂: Correlation Between Photoreactivity and Charge Carrier Recombination Dynamics." *J. Phys. Chem.*, **98** 13669–13679 (1994)
28. Premaratne, WAPJ, Rowson, NA, "Microwave Assisted Dissolution of Sri Lankan Ilmenite: Extraction and Leaching Kinetics of Titanium and Iron Metals." *J. Sci. Univ. Kelaniya*, **9** 1–14 (2015)
29. Jaimy, KB, Vidya, K, Saraswathy, HUN, Hebalkar, NY, Warriar, KGK, "Dopant-Free Anatase Titanium Dioxide as Visible-Light Catalyst: Facile Sol-Gel Microwave Approach." *J. Environ. Chem. Eng.*, **3** (2) 1277–1286 (2015)
30. Begum, NS, Ahmed, HMF, Gunashekar, KR, "Effect of Ni Doping on Photocatalytic Activity of TiO₂ Thin Films Prepared by Liquid Phase Deposition Technique." *Bull. Mater. Sci.*, **31** (5) 747–751 (2008)
31. Hong, YC, Bang, CU, Shin, DH, Uhm, HS, "Band Gap Narrowing of TiO₂ by Nitrogen Doping in Atmospheric Microwave Plasma." *Chem. Phys. Lett.*, **413** 454–457 (2005)
32. Ganesh, I, Gupta, AK, Kumar, PP, Sekhar, PSC, Radha, K, Padmanabham, G, Sundararajan, G, "Preparation and Characterization of Ni-doped TiO₂ Materials for Photocurrent and Photocatalytic Applications." *Sci. World J.*, 1–16 (2012)
33. Lakachew, A, *Synthesis of Ni-N Co-Doped TiO₂ Nanoparticles and Their Photocatalytic Activity for Rhodamine-B Degradation*. Haramaya University, Thesis (2011)
34. Asahi, R, Morikawa, T, Ohwaki, T, Aoki, K, dan Taqa, Y, "Visible Light Photocatalysis in Nitrogen Doped in Titanium Dioxide." *Science*, **293** (5528) 269–271 (2001)
35. Zhang, J, Wu, Y, Xing, M, Leqhari, SAK, Sajjad, S, "Development of Modified N Doped TiO₂ Photocatalyst with Metals, Nonmetals and Metal Oxides." *Energy Environ. Sci.*, **3** 715–726 (2010)
36. Dimitrakupoulou, D, Rethemiotaki, I, Frontistis, Z, Xekoukoulotakis, NP, Venieri, D, Mantzavinou, D, "Degradation, Mineralization and Antibiotic Inactivation of Amoxicillin by UV-A/TiO₂ Photocatalysis." *J. Environ. Manag.*, **98** (1) 168–174 (2012)